Published in final edited form as:
Biomaterials. 2010 November ; 31(31): 7883–7891. doi:10.1016/j.biomaterials.2010.07.013.

A silk platform that enables electrophysiology and targeted drug delivery in brain astroglial cells

Valentina Benfenati[1,*], **Stefano Toffanin**[1,*], **Raffaella Capelli**[1,*], **Laura M. A. Camassa**[2], **Stefano Ferroni**[3], **David L. Kaplan**[4], **Fiorenzo G. Omenetto**[4], **Michele Muccini**[1], and **Roberto Zamboni**[1]

[1]Consiglio Nazionale delle Ricerche (CNR), Istituto per lo Studio dei Materiali Nanostrutturati (ISMN), via Gobetti, 101, 40129, Bologna, Italy

[2]Centre for Molecular Biology and Neuroscience, University of Oslo, P.O. Box 1105 Blindern NO-0317 Oslo, Norway

[3]Department of Human and General Physiology, University of Bologna, via S.Donato 19/2, 40127, Bologna, Italy

[4]Department for Biomedical Engineering, Tufts University, Medford, MA 02155, USA

Abstract

Astroglial cell survival and ion channel activity are relevant molecular targets for the mechanistic study of neural cell interactions with biomaterials and/or electronic interfaces. Astrogliosis is the most typical reaction to *in-vivo* brain implants and needs to be avoided by developing biomaterials that preserve astroglial cell physiological function. This cellular phenomenon is characterized by a proliferative state and altered expression of astroglial potassium (K^+) channels. Silk is a natural polymer with potential for new biomedical applications due to its ability to support in vitro growth and differentiation of many cell types. We report on silk interactions with cultured neocortical astroglial cells. Astrocytes survival is similar when plated on silk-coated glass and on poly-D-lysine (PDL), a well-known polyionic substrate used to promote astroglial cell adhesion to glass surfaces. Comparative analyses of whole-cell and single-cell patch-clamp experiments reveal that silk- and PDL-coated cells display depolarized resting membrane potentials (~ -40 mV), very high input resistance, and low specific conductance, with values similar to those of undifferentiated glial cells. Analysis of K^+ channel conductance reveals that silk-astrocytes express large outwardly delayed rectifying K^+ current (K_{DR}). The magnitude of K_{DR} in PDL- and silk-coated astrocytes is similar, indicating that silk does not alter the resting K^+ current. We also demonstrate that guanosine-(GUO) embedded silk enables the direct modulation of astroglial K^+ conductance in vitro. Astrocytes plated on GUO-embedded silk are more hyperpolarized and express inward rectifying K^+ conductance (K_{ir}). The K^+ inward current increase and this is paralleled by upregulation and membrane-polarization of K_{ir}4.1 protein signal. Collectively these results indicate that silk is a suitable biomaterial platform for the in vitro studies of astroglial ion channel responses and related physiology.

Corresponding author information: Valentina Benfenati, CNR-ISMN via Gobetti, 101, 40129, Bologna, Italy, v.benfenati@bo.ismn.cnr.it, Tel 00 39 051 6398527, Fax 00 39 051 6398540, Mobile: 00 39 338 9090046.
*These authors equally contributes to this work

1. Introduction

Biomaterials that enable the control of bioelectrical signals in neural cells have great potential for use in tissue engineering, targeted drug release or stem cell based neuroregenerative medicine [1,2]. Ion channels as well as electrical signalling between excitable cells are well known, and their function in non-excitable (glial) cells, have recently been of interest. Several studies indicate a role for astroglial ion channels in different brain cell functions, including proliferation, differentiation and neurogenesis [3,4]. Furthermore, astrocytes, the most numerous cell type in the brain, tightly regulate homeostasis [5,6]. At the cellular level, astroglial equilibration of external ion composition and osmotic gradients is controlled by selective transmembrane movement of inorganic and organic molecules and the osmotically driven flux of water [5]. Thus, astroglial ion channels exert crucial functions in the physiology of the Central Nervous System (CNS) [6].

Astrocytes express different types of voltage-gated ion channels [7], including voltage dependent potassium (K^+) conductance, which were identified both *in vitro* and *in vivo*. Delayed rectifying K^+ channel (K_{DR}) and members of inward rectifying K^+ channels (K_{ir}) are mainly involved in maintenance of astroglial resting membrane potential and in astroglial control of extracellular K^+ homeostasis [8-10]. The physiological relevance of these astroglial K^+ conductance resides, in their pivotal role in the clearance of extracellular K^+ accumulation, which is crucial for the maintenance of neuronal signalling. Neuronal activity leads to an efflux of K^+ ions which is counteracted by uptake from astroglial cells [10]. This process, often referred to as "spatial K^+ buffering"[11], redistributes the excess K+ ions from the active neurophil towards sinks of the brain extracellular fluids by mean of K^+ channels, in particular the inwardly rectifying potassium channel $K_{ir}4.1$ [11,12].

Moreover, astroglial ion channel expression and activity are dynamically regulated [13,14]. In response to acute brain injury or pathophysiological conditions, astrocytes undergo dramatic alterations in properties, referred to as gliosis [15,16]. The latter is characterized by activation of the proliferative state, release of growth and trophic factors, and loss of homeostatic functions [16]. Numerous *in vivo* studies revealed that, following various brain insults, K+ channels in astroglial cells are altered at the lesion site where reactive gliosis occurs [17-19]. Moreover, it has recently been shown that in primary brain tumors such as gliomas, K^+ conductance acts in concert with chloride ion channels to promote cell invasion and the formation of brain metastasis [19,20]. Finally, modulation of bioelectrical activity of glial derived stem cells has been suggested as a target to pivot proper stem cell differentiation to counteract neurodegeneration [2]

All of this evidence indicates that monitoring and controlling astroglial cell ion channel function is relevant to define mechanistic relationships between cell-substrate interactions *in vitro* and to control gliotic reactions induced by prostheses intended for the Central Nervous System [21]

Silks are natural protein polymers that have been used clinically as sutures for centuries. In recent years, silk fibroin has been extensively studied for new biomedical applications, such as functional tissue engineering and drug delivery [22,23], due to its biocompatibility, slow degradability and remarkable mechanical properties. Silk fibroin in various formats (films, fibers, nets, meshes, membranes, gels, sponges) supports adhesion, proliferation, and differentiation in vitro of different cell types [24,25]. Concerning brain cells, recent studies indicate that silk has good compatibility for growing hippocampal neurons [26]. Glial Fibrillar Acid Protein (GFAP) positive cells (a well known astroglial protein marker) derived from the differentiation of brain stem cells, grew on silk coated plastic with a rate comparable to that observed for collagen [27]. Neural cell biocompatibility *in vitro* was mainly based on the of

expression of neuronal and glial trophic and growing factors [26-28]. However, the effects of silk on astroglial ion channel expression and function, and in turn on bioelectrical passive membrane properties of glial cells (like resting membrane potential and membrane resistance), that are critical for defining the functional state of the astroglial syncytium are not known.

The goal of the present study was to assess the effects of silk on astroglial ion-channel activity. In particular we focus on the analyses of expression and properties of K^+ conductance expressed by pure rat neocortical astroglial primary cultures that had been previously shown to be involved in astroglial physiology and pathophysiology [6,7,29,30]. The electrophysiological characteristics of silk-films plated astrocytes were compared with those of poly-D-lysine (PDL) seeded cells, a well known poly-ionic substrate employed for *in vitro* astroglial cell culture [31]. Subsequently, we sought to modulate K^+ conductance *in vitro*, plating astrocytes on silk films embedded with trophic factor guanosine (GUO).

Methods

2.1 Cell culture

Primary cultures of pure cortical rat astrocytes were prepared as described previously [30]. Briefly, cerebral cortices devoid of meninges were triturated and placed in cell culture flasks containing Dulbecco's modified Eagle's medium (DMEM)–glutamax medium with 15% fetal bovine serum (FBS) and penicillin–streptomycin (100 U/mL and 100 lg/mL respectively) (Gibco-Invitrogen, Milan, Italy). Culture flasks were maintained in a humidified incubator with 5% CO_2 for 2–5 weeks. Immunostaining for glial fibrillary acidic protein (GFAP) and the flat, polygonal morphological phenotype of the cultured cells indicated that more than 95% were type 1 cortical astrocytes [54]. At confluence, astroglial cells were enzymatically dispersed using trypsin–EDTA in poly-D-lysine coated of SF coated glass coverslips (19 mm diameter) at a density of 1×10^4 per dish and maintained in culture medium containing 15% FBS.

2.2 Preparation of silk solution and films

Silk solutions were prepared from *Bombyx mori* silkworm cocoons (supplied by Tajima Shoji, Co., Yokohama, Japan) according to the procedures described in our previous studies [32]. The cocoons were degummed in boiling 0.02-M Na_2CO_3 (Sigma-Aldrich, St Louis, Mo) solution for 30 min. The fibroin extract was then rinsed three times in Milli-Q water, dissolved in a 9.3-M LiBr solution yielding a 20% (w/v) silk protein solution, and subsequently dialyzed (dialysis membranes, MWCO 3,500) against distilled water for 2 days to obtain a pure silk aqueous solution (ca. 8 wt/vol %). Eight percent silk solution was filtered twice through 0.2 μm Millipore filters (Sarsted) to generate a sterile solution. For film preparation, a 160 μl aliquot of 8% silk solution was cast on 19 mm diameter glass coverslips, to generate films with a thickness of around 20 μm [32]. The as-cast silk films were desiccated for 4 h in a sterile hood. The silk-coated glass coverlips were placed in a 35 mm Petri dishes and covered with a drop of (DMEM)–glutamax medium with 10% fetal bovine serum (FBS) and penicillin–streptomycin (100 U/mL and 100 lg/mL, respectively), and left in the incubator overnight. The next day astrocytes were replated in Petri dishes as described above. To prepare silk+GUO films, a 500 μM silk guanosine solution was prepared by diluting GUO stock solution 1:400 in the 8% silk solution. Silk+GUO films were prepared following the same procedure used for pure silk fims.

2.3 Cell viability and counting

Astrocytes plated on the different coverslips were mounted in a custom made perfusion chamber and incubated for 5 min with Cell trace assay (Invitrogen) or with fluorescein diacetate (Sigma Aldrich) with DAPI. After rinsing with physiological saline solution a sequence of confocal images (5 to 8 different fields of 0.2 × 0.2 mm for each sample) was taken using a

Nikon TE 2000 inverted confocal microscope (40× oil-objective). Living cells were counted and number of cells/mm^2 was calculated and compared at each time point analyzed.

2.4 Immunofluorescence

Astrocytes plated on different coverslips were fixed with 4% p/v paraformaldehyde in 0.1 M phosphate-buffered saline (PBS) for 15 min. After blocking with 3% bovine serum albumin (BSA) in PBS for 15 min at room temperature (20–24°C), cells were incubated overnight with rabbit anti-K_{ir}4.1 (Alomone Labs, Israel) or mouse-anti-GFAP (Sigma-Aldrich, Milan, Italy) affinity-purified antibodies diluted 1:100 in blocking solution to which 0.1% Triton X100 was added. After rinsing with blocking solution cells were incubated, respectively, with Alexa Fluor 595-conjugated donkey anti-rabbit or Alexa Fluor 595-conjugated donkey anti-rabbit antibodies (Molecular Probes-Invitrogen, Carlsbad, CA, USA) diluted 1:1000 in blocking solution containing 0.1% Triton X100. Coverslips were next mounted with Prolong Anti-Fade (Molecular Probes-Invitrogen) and optically imaged with a Nikon TE 2000 inverted confocal microscope equipped with a 40× oil-objective and 400 nm diode, 488 nm Ar^+ and 543 nm He-Ne lasers as exciting sources.

2.5 Electrophysiology

Current recordings were obtained with the whole-cell configuration of the patch clamp technique [33]. Patch pipettes were prepared from thin-walled borosilicate glass capillaries to have a tip resistance of 2-4 MΩ when filled with the standard internal solution. Membrane currents were amplified (List EPC-7) and stored on a computer for off-line analysis (pClamp 6, Axon Instrument and Origin 6.0, MicroCal). Because of the large current amplitude, the access resistance (below 10 MΩ) was corrected 70-90%. Experiments were carried out at room temperature (20-24°C).

2.6 Solutions and chemicals

All salts and chemicals employed for the investigations were of the highest purity grade (Sigma). For electrophysiological experiments the standard bath saline was (mM): 140 NaCl, 4 KCl, 2 $MgCl_2$, 2 $CaCl_2$, 10 HEPES, 5 glucose, pH 7.4 with NaOH and osmolarity adjusted to ~315 mOsm with mannitol. The intracellular (pipette) solution was composed of (mM): 144 KCl, 2 $MgCl_2$, 5 EGTA, 10 HEPES, pH 7.2 with KOH and osmolarity ~300 mOsm. When using external solutions with different ionic compositions, salts were replaced equimolarly. The different salines containing pharmacological agents were applied with a gravity-driven, local perfusion system at a flow rate of ~200 μl/min positioned within ~100 μm of the recorded cell. Guanosine was dissolved in NaOH 1N and the final concentration of NaOH in culture dishes was 0.01%.

2.7 Statistical Methods

Results were statistically analyzed using one-way analysis of variance (ANOVA) or Independent t student test. A statistically significant difference was reported if $p < 0.05$ or less. Data are reported as the mean ± standard error (SE) from at least three separate experiments.

3 Results and Discussion

3.1 Pure neocortical astroglial cell growth on silk substrates

Long-term biocompatibility of prostheses intended for the Central Nervous System depends to a large extent on the modulation of gliosis, a tissue-level response to injury that involves the activation of various types of cells including astrocytes. In its final form this response is composed of reactive astrocytes that undergo migration, hypertrophy, proliferation, clustering, and formation of dense interweaving processes to form an impenetrable mechanical barrier to

contain the damaged site [15,16]. Evaluation of long term astroglial cell reactions to biomaterials has been considered an important biocompatibility assessment [21]. Thus, in order to define the viability and growth of astroglial cells on the silk substrate, pure rat neocortical astroglial cells were plated on poly-D-lysine (PDL), a well-known substrate used to promote cell adhesion *in vitro* for primary brain cells [31], and on silk coated-glass coverslips. After 48 h, 96 h and 21d from re-plating viability assays were performed (Fig 1E). Single plane confocal imaging analyses depicts viable astrocytes plated on both PDL and silk (Fig 1 A-B). Importantly, morphological observation revealed that a polygonal flat shape typical of *in vitro* cultured primary astrocytes [31] was maintained in silk plated astrocytes. Hystogram plot of cell counting at different time point indicated that survival of astrocytes plated on silk was comparable to those observed in PDL-plated cells (Fig 1 E).

Reactive astrocytes are identified as cells with upregulated expression of intermediate filament proteins such as glial fibrillary acidic protein (GFAP), a well known protein marker of astroglial cells *in vivo* and *in vitro* [15]. We thus performed immunofluorescent GFAP staining and confocal imaging of the PDL and silk grown cells (Fig 1 C-D). Micrograph analyses of immunofluorescent staining intensity confirmed that almost 95% were astrocytes [30] and revealed a similar expression level of GFAP on both substrates.

These results support the finding previously reported for embryonic stem cell-derived glial precursor cells grown on silk, indicating that silk is a good substrate for glial cell growth [27]. However, in this prior study cell proliferation was higher and metabolic activity lower on collagen type 1 and poly-ornithine substrates when compared to silk substrate, whereas we did not find differences in survival of the cells plated on silk and on PDL-coated substrates. Moreover, morphological observation and expression levels of GFAP were not enhanced in the cells cultured on the silk, suggesting that silk does not promote gliotic reactions, *in vitro*.

3.2 Electrophysiological studies of astroglial cells on silk

The main goal in this study was to verify the effect of silk on astroglial K^+channels that are known to be involved in the physiology and pathophysiology of CNS. To this end whole-cell patch-clamp experiments were performed on cells at low density, 3d after replating on silk and on PDL. With control intracellular and extracellular saline, cells were voltage clamped at a holding potential (V_h) of -60 mV and, after stepping to -120 mV for 400 ms, a slow ramp (180 mV/600 ms) from -120 to 60 mV (inset in Fig. 3) was applied to evoke whole-cell currents. Current amplitude was recorded and passive membrane properties were calculated (Fig 2). The resting membrane potentials (V_{mem}) of silk-coated and PDL cells were comparable with values of -32 ± 3 mV in PDL-plated and -32 ± 2 mV in the silk-plated cells (Fig 2A). Accordingly, no significant changes were observed in the input resistance values (1348 ± 208 MΩ in PDL-astrocytes, 1744 ± 279 MΩ in SF-coated cells, Fig 2B). As an additional indication that silk did not modify astroglial cell morphology in cells seeded at low concentration, capacitance as an indication of cell-surface area of silk plated astrocytes was not different from the PDL cells (61 ± 8 pF for PDL-plated astrocytes; 56 ± 3 pF for silk-plated cells). The specific conductance (spG; 0.017± 0.004 ns/pF for silk cells and 0.014±0.002 for PDL) recorded at -60 mV were also similar.

Importantly, the data we report on passive membrane properties of astrocytes plated on PDL and on silk resemble those of previous studies with primary astroglia plated on poly-styrene Petri dishes. Silk and PDL-plated cells displayed intact depolarized resting membrane potentials (Fig 2A), high input resistance (Fig 2C) and low specific conductance (Fig 2D) [29,30,34].

Typical current traces elicited by the ramp current protocol described above (inset in Fig 3) in PDL- and silk-plated astrocytes are shown in Figure 3. The ramp current traces displayed a

strong outward rectification as witnessed by the negligible currents recorded at membrane potentials more hyperpolarized than -40 mV in PDL (Fig 3A) as well as silk-plated (Fig 3B) astrocytes. Importantly, current density recorded at -120 mV and +60 mV was not significantly different for silk and PDL-plated cells (-1.8 ± 0.5 pA/pF at -120 mV and 35.1 ±7,2 at +60 mV for PDL (n=10); -1.6 ± 0.4 pA/pF at -120 mV and 36.3 ± 5.6 at +60 mV for silk (n=11)).

To analyze voltage- and time-dependencies of conductance expressed by PDL- and silk-plated cells, astrocytes were stimulated with 500-ms voltage steps (V_h = -60 mV) from -120 to 60 mV in 20mV increments (inset of Fig 4 A). Representative current traces obtained on PDL- and silk-astrocytes in response to the applied voltage are displayed in Fig 4 (A-B). Rapidly activating, non-inactivating, voltage-dependent whole-cell currents were elicited with the family of voltage-step protocols at potentials positive to -40 mV (Fig 4 A-B). Time- and voltage-dependent analyses obtained by I/V plot of mean steady-state and peak-current density values recorded for each voltage step (Fig 4 C-D) revealed similar biophysical features of cell current on silk and PDL.

All the data indicate that silk-plated astrocytes have voltage-gated K^+ channels activated at membrane potentials more positive than -40 mV. The biophysical properties that we recorded overlap those of K_{DR} previously characterized in immature glial cells identified for astrocytes plated directly on polystyrene Petri dishes or by mean of PDL or poly-ornitine [29,35,36]. These results demonstrate that silk does not alter K^+ conductance of astroglial cells *in vitro*, and hence is a suitable biomaterial for electrophysiological studies of astroglial cells.

3.3 Silk-enabled ion channel targeted drug delivery to astroglial cells

Because of the importance of studying dynamic modulation of astroglial K^+ channels expression, previous studies aimed at identifying protocols to modulate/activate glial K^+conductance *in vitro*, by adding pharmacological compounds to the culture media [29,30, 36]. In particular we have shown that after prolonged (48 h) treatment with GUO, astrocytes acquired large K_{ir} conductance, which is not expressed in standard culture conditions. The conductance increase was paralleled by an increase in K_{ir}4.1 protein channel expression [29]. In order to assess silk as vehicle for the delivery of compounds to modulate astroglial K^+ conductance *in vitro*, silk containing 500 μM GUO (silk+GUO) was prepared and astrocytes were replated on silk and on silk+GUO plates. After 48 hr from replating, whole-cell patch clamp experiments were carried out and comparative analyses was obtained with silk and silk +GUO plated cells. The astrocytes plated on silk+500 μM GUO for 48 hrs displayed significant changes in membrane properties (Fig 5 A-B, n=27 for silk, and n=22 for silk+GUO). In particular, V_{mem} was more hyperpolarized (~ -60 mV) in silk+GUO cells compared to pure silk, with a significant decrease in input resistance (Fig 5A, 1575±160 MΩ for silk, 688±175 MΩ for silk+GUO $p<0.01$) accompanied by a 5-fold increase in specific conductance (Fig 5B, 0,017±0,00287 nS/pF for silk; 0,072±0,012 nS/pF for silk+GUO $p<0.01$). The typical current profile of a 48-hr silk+GUO astrocyte, in response to the applied voltage ramp protocol, is shown in Fig. 5D. Compared to currents recorded in silk cells the same days (Fig 5C), the current traces elicited in silk+GUO astrocytes showed a double rectification profile with large inward currents activated at membrane potentials more negative than -40 mV (Fig 5D, arrow). Moreover, differently from astrocyte on silk, in cells plated on silk+GUO the voltage-step protocol (inset in Fig 4A), induced inward currents at negative membrane potentials (fully activated within 50 ms) and did not show any time-dependent inactivation. (compare Fig 5E with F, also Fig 4B). It was previously shown that barium selectively blocks K_{ir} channels in cultured astrocytes [37,38]. The inward current of silk+GUO cells was inhibited by submillimolar concentrations (200 μM) of barium (Ba^{2+}), as indicated by IV plot in Fig H, whereas the current response in silk cells was not affected by barium. Note that part of the

outward current was also sensitive to Ba^{2+} application, suggesting a weak-rectifying nature of the K_{ir} conductance [38].

The data suggest that K_{ir} conductance is responsible for mediating at least part of the up-regulated conductance in silk+GUO cells. Therefore, we performed immunofluoresence confocal analyses to determine the expression of K_{ir} 4.1 (the protein channel that underlies astroglial K_{ir} conductance *in vivo* [39] in silk and silk+GUO embedded cells. The single plane confocal images in Figure 6 are representative of the data obtained for K_{ir}4.1 staining in silk cells (Fig 6A) and silk+GUO cells (Fig 6B). An increase of ~50% in fluorescent signal was observed in the silk+GUO cells, confirmed by fluorescence intensity analysis reported in Fig 6 E-F. High magnification images indicated that the expression pattern of K_{ir}4.1 was mislocalized in silk cells (Fig 6C), whereas a more polarized expression pattern on astroglial plasma-membranes was detectable in the silk+GUO cells (Fig 6 D, arrows)

Extracellular nucleotides and nucleosides are a class of signalling molecules that play critical roles both in physiological conditions and in the pathophysiology of several neurodegenerative disorders [40]. The cellular and molecular mechanisms underlying the activity of adenine-based nucleotides and nucleosides on both neuronal and glial cells have been well characterized [40]. Local cell-mediated adenosine release has been demonstrated to represent an effective strategy to suppress seizures in the rat-kindling model of epilepsy [41]. Of note, silk has been recently employed as cell-based drug delivery vehicle for adenosine-based therapies against epileptic seizures [42].

A major role of the guanine nucleoside guanosine in neuroprotection has been underscored [43]. The importance of GUO as a protective molecule is further supported by *in vivo* findings indicating that chronically administered GUO prevented the development of seizures and cell death in a model of glutamate excitotoxicity [44]. In our previous study, considering the well-known physiological role of K_{ir} conductance, we addressed the question whether K_{ir} channels are a molecular target of the neuroprotective effect of guanosine [29]. In the present work we corroborated our hypothesis since we found that cells plated on GUO embedded silk films expressed barium sensitive K_{ir}, with biophysical features resembling those of K_{ir}4.1 as previously described [29,37]. Moreover, we have identified a new method to obtain rapid "functional" differentiation of astroglial cells i*n vitro*. Indeed, previous studies aimed at obtaining the same outcome by the addition of dbcAMP to the cell media verified that long term treatment (1-2 weeks) was required for example to induce K_{ir} current or ClC current in primary astroglial cells [30]. In glial cells from humans suffering from pharmacoresistant temporal lobe epilepsy there is also a reduction in K_{ir} density and inward rectification, which probably contributes to seizure generation owing to a defect in the regulation of extracellular K^+ homeostasis [45]. Thus, direct modulation of K_{ir} astroglial conductance could represent an alternative pathway for more sophisticated and targeted therapies against epilepsy. Considering the well known biocompatibility of silk as a drug delivery vehicle, possible *in vivo* applications of drug release in the context of epilepsy therapies can be considered [14,42,45].

5. Conclusions and Perspectives

Collectively the data presented indicate that silk is a favourable substrate to support the in vitro growth of primary rat neocortical cells, even in long term culture (three weeks *in vitro*). Comparative quantitative analyses of biophysical properties and of current density of K_{DR}-current revealed no significant differences between PDL and silk coated astrocytes. Since there is no silk-induced affect on the K^+ current in astrocytes, we conclude that silk serves as a suitable "bioelectrical" compatible substrate for studying brain astroglial ion channels *in vitro*. Considering the well-known *in vivo* protective effect of GUO [40,43], silk offers a platform to implement a strategy for targeted molecular drug delivery to brain astroglial cells.

The results of the present study have implications for regenerative medicine, as stem cell differentiation is known to be correlated to resting membrane potential and K^+ channel activity or expression pattern [2]. It would be thus interesting to verify if the same effect of upregulation of $K_{ir}4.1$ in GUO-embedded cells could be obtained with embryonic stem cells.

Acknowledgments

This work has been supported by EU projects PF6 035859-2 (BIMORE) and FP7-ICT- 248052 (PHOTO-FET). We also would like to thank the NIH P41 Tissue Engineering Resource Center (P41 EB002520) for partial financial support.

References

1. Xu T, Molnar P, Gregory C, Das M, Boland T, Hickman JJ. Electrophysiological characterization of embryonic hippocampal neurons cultured in a 3D collagen hydrogel. Biomaterials 2009;30:4377–4383. [PubMed: 19501396]
2. Sundelacruz S, Levin M, Kaplan DL. Role of membrane potential in the regulation of cell proliferation and differentiation. Stem Cell Rev 2009;5:231–246. [PubMed: 19562527]
3. Kressin K, Kuprijanova E, Jabs R, Seifert G, Steinhauser C. Developmental regulation of Na+ and K + conductances in glial cells of mouse hippocampal brain slices. Glia 1995;15:173–187. [PubMed: 8567069]
4. Habela CW, Olsen ML, Sontheimer H. ClC3 is a critical regulator of the cell cycle in normal and malignant glial cells. J Neurosci 2008;28:9205–9217. [PubMed: 18784301]
5. Benfenati V, Ferroni S. Water transport between CNS compartments: functional and molecular interactions between aquaporins and ion channels. Neuroscience 2010;168:926–940. [PubMed: 20026249]
6. Simard M, Nedergaard M. The neurobiology of glia in the context of water and ion homeostasis. Neuroscience 2004;129:877–896. [PubMed: 15561405]
7. Verkhratsky A, Steinhäuser C. Ion channels in glial cells. Brain Res Brain Res Rev 2000;32:380–412. [PubMed: 10760549]
8. Orkand RK, Nicholls JG, Kuffler SW. Effect of nerve impulses on the membrane potential of glial cells in the central nervous system of amphibia. J Neurophysiol 1966;29:788–806. [PubMed: 5966435]
9. Walz W. Role of astrocytes in the clearance of excess extracellular potassium. Neurochem Int 2000;36:291–300. [PubMed: 10732996]
10. Kofuji P, Newman EA. Potassium buffering in the central nervous system. Neuroscience 2004;129:1045–1056. [PubMed: 15561419]
11. Kofuji P, Ceelen P, Zahs KR, Surbeck LW, Lester HA, Newman EA. Genetic inactivation of an inwardly rectifying potassium channel (Kir4.1 subunit) in mice: phenotypic impact in retina. J Neurosci 2000;20:5733–5740. [PubMed: 10908613]
12. Olsen ML, Sontheimer H. Functional implications for Kir4.1 channels in glial biology: from K+ buffering to cell differentiation. J Neurochem 2008;107:589–601. [PubMed: 18691387]
13. Somjen GG. Ion regulation in the brain: implications for pathophysiology. Neuroscientist 2002;8:254–267. [PubMed: 12061505]
14. Seifert G, Schilling K, Steinhäuser C. Astrocyte dysfunction in neurological disorders: a molecular perspective. Nat Rev Neurosci 2006;7:194–206. [PubMed: 16495941]
15. Calvo JL, Carbonell AL, Boya J. Co-expression of glial fibrillary acidic protein and vimentin in reactive astrocytes following brain injury in rats. Brain Res 1991;566:333–336. [PubMed: 1814551]
16. Chvátal A, Anderová M, Neprasová H, Prajerová I, Benesová J, Butenko O, et al. Pathological potential of astroglia. Physiol Res 2008;57:S101–S110. [PubMed: 18481910]
17. D'Ambrosio R, Maris DO, Grady MS, Winn HR, Janigro D. Impaired K+ homeostasis and altered electrophysiological properties of post-traumatic hippocampal glia. J Neurosci 1999;19:8152–8162. [PubMed: 10479715]
18. Bordey A, Hablitz JJ, Sontheimer H. Reactive astrocytes show enhanced inwardly rectifying K+ currents in situ. Neuroreport 2000;11:3151–3155. [PubMed: 11043540]

19. Higashimori H, Sontheimer H. Role of Kir4.1 channels in growth control of glia. Glia 2007;55:1668–1679. [PubMed: 17876807]
20. Sontheimer H. An unexpected role for ion channels in brain tumor metastasis. Exp Biol Med 2008;233:779–791.
21. Polikov VS, Tresco PA, Reichert WM. Response of brain tissue to chronically implanted neural electrodes. J Neurosci Methods 2005;148:1–18. [PubMed: 16198003]
22. Altman GH, Diaz F, Jakuba C, Calabro T, Horan RL, Chen J, Lu H, Richmond J, Kaplan DL. Silk-based biomaterials. Biomaterials 2003;24:401–416. [PubMed: 12423595]
23. Hofmann S, Foo CT, Rossetti F, Textor M, Vunjak-Novakovic G, Kaplan DL, et al. Silk fibroin as an organic polymer for controlled drug delivery. J Control Release 2006;111:219–227. [PubMed: 16458987]
24. Inouye K, Kurokawa M, Nishikawa S, Tsukada M. Use of Bombyx mori silk fibroin as a substratum for cultivation of animal cells. J Biochem Biophys Methods 1998;37:159–164. [PubMed: 9870190]
25. Wang Y, Kim HJ, Vunjak-Novakovic G, Kaplan DL. Stem cell-based tissue engineering with silk biomaterials. Biomaterials 2006;27:6064–6082. [PubMed: 16890988]
26. Tang X, Ding F, Yang Y, Hu N, Wu H, Gu X. Evaluation on in vitro biocompatibility of silk fibroin-based biomaterials with primarily cultured hippocampal neurons. J Biomed Mater Res A 2009;91:166–174. [PubMed: 18780373]
27. Uebersax L, Fedele DE, Schumacher C, Kaplan DL, Merkle HP, Boison D, Meinel L. The support of adenosine release from adenosine kinase deficient ES cells by silk substrates. Biomaterials 2006;27:4599–4607. [PubMed: 16709437]
28. Yang Y, Chen X, Ding F, Zhang P, Liu J, Gu X. Biocompatibility evaluation of silk fibroin with peripheral nerve tissues and cells in vitro. Biomaterials 2007;28:1643–1652. [PubMed: 17188747]
29. Benfenati V, Caprini M, Nobile M, Rapisarda C, Ferroni S. Guanosine promotes the upregulation of inward rectifier potassium current mediated by Kir4.1 in cultured rat cortical astrocytes. J Neurochem 2006;98:430–445. [PubMed: 16805837]
30. Ferroni S, Marchini C, Schubert P, Rapisarda C. Two distinct inwardly rectifying conductances are expressed in long term dibutyryl-cyclic-AMP treated rat cultured cortical astrocytes. FEBS Lett 1995;367:319–325. [PubMed: 7607331]
31. Lascola CD, Kraig RP. Whole-cell chloride currents in rat astrocytes accompany changes in cell morphology. J Neurosci 1996;16:2532–2545. [PubMed: 8786429]
32. Lawrence BD, Omenetto F, Chui K, Kaplan DL. Processing methods to control silk fibroin film biomaterial features. J Mater Sci 2008;43:6967–6985.
33. Hamill OP, Marty, Neher E, Sackmann B, Sigworth FJ. Improved patch-clamp tecniques for high resolution current recording from cells and cell free membrane patches. Pflügers Archiv 1981;391:85–100.
34. Olsen ML, Sontheimer H. Mislocalization of Kir channels in malignant glia. Glia 2004;46:63–73. [PubMed: 14999814]
35. Bordey A, Sontheimer H. Differential inhibition of glial K(+) currents by 4-AP. J Neurophysiol 1999;82:3476–3487. [PubMed: 10601476]
36. Noël G, Belda M, Guadagno E, Micoud J, Klöcker N, Moukhles H. Dystroglycan and Kir4.1 coclustering in retinal Müller glia is regulated by laminin-1 and requires the PDZ-ligand domain of Kir4.1. J Neurochem 2005;94:691–702. [PubMed: 16033419]
37. Ransom CB, Sontheimer H. Biophysical and pharmacological characterization of inwardly rectifying K+ currents in rat spinal cord astrocytes. J Neurophysiol 1995;73:333–346. [PubMed: 7714576]
38. Nichols CG, Lopatin AN. Inward rectifier potassium channels. Ann Rev Physiol 1997;59:171–191. [PubMed: 9074760]
39. Nagelhus EA, Horio Y, Inanobe A, Fujita A, Haug FM, Nielsen S, et al. Immunogold evidence suggests that coupling of K+ siphoning and water transport in rat retinal Müller cells is mediated by a coenrichment of Kir4.1 and AQP4 in specific membrane domains. Glia 1999;26:47–54. [PubMed: 10088671]
40. Neary JT, Rathbone MP, Cattabeni F, Abbracchio MP, Burnstock G. Trophic actions of extracellular nucleotides and nucleosides on glial and neuronal cells. Trends Neurosci 1996;19:13–18. [PubMed: 8787135]

41. Boison D, Stewart KA. Therapeutic epilepsy research: from pharmacological rationale to focal adenosine augmentation. Biochem Pharmacol 2009;78:1428–1437. [PubMed: 19682439]

42. Szybala C, Pritchard EM, Lusardi TA, Li T, Wilz A, Kaplan DL, et al. Antiepileptic effects of silk-polymer based adenosine release in kindled rats. Exp Neurol 2009;219:126–135. [PubMed: 19460372]

43. Rathbone MP, Middlemiss PJ, Gysbers JW, Andrew C, Herman MA, Reed JK, et al. Trophic effects of purines in neurons and glial cells. Prog Neurobiol 1999;59:663–690. [PubMed: 10845757]

44. Vinadè ER, Schmidt AP, Frizzo ME, Izquierdo I, Elisabetsky E, Souza DO. Chronically administered guanosine is anticonvulsant, amnesic and anxiolytic in mice. Brain Res 2003;977:97–102. [PubMed: 12788518]

45. Hinterkeuser S, Schroder W, Hager G, Seifert G, Blumcke I, Elger CE, et al. Astrocytes in the hippocampus of patients with temporal lobe epilepsy display changes in potassium conductances. Eur J Neurosci 2000;12:2087–2096. [PubMed: 10886348]

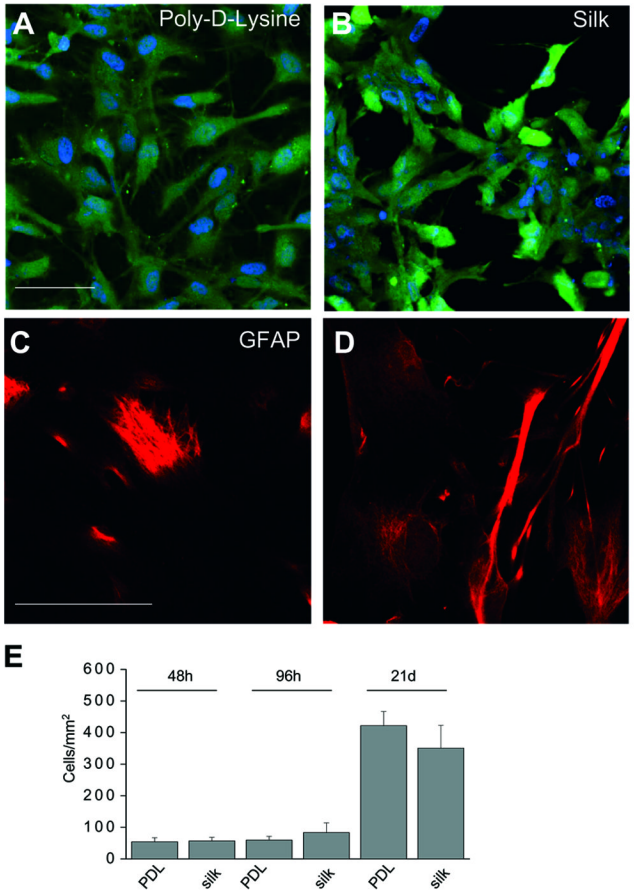

Figure 1.

A-B) Single plane confocal image of Cell trace assay (green) and DAPI staining (blu) of astrocytes plated in poly-D-Lysine (A) and silk (B). The morphology of astrocytes was not different in the two experimental conditions. C-D) Single plane 40× confocal image of GFAP staining of cells plated on poly-D-Lysine glass coverslip (C) and silk-coated astrocytes (D). Almost 95% of the cells were astrocytes. Of note GFAP immunosignal was not different in intensity in both experimental conditions. Scale bar is 50 μm. E) Histogram plot of mean cell counts after 48 hrs, 96 hrs and 21d after replating astrocytes on PDL and silk. Note that no significant difference was observed in cell viability at each time point ($p>0.05$, independent t test).

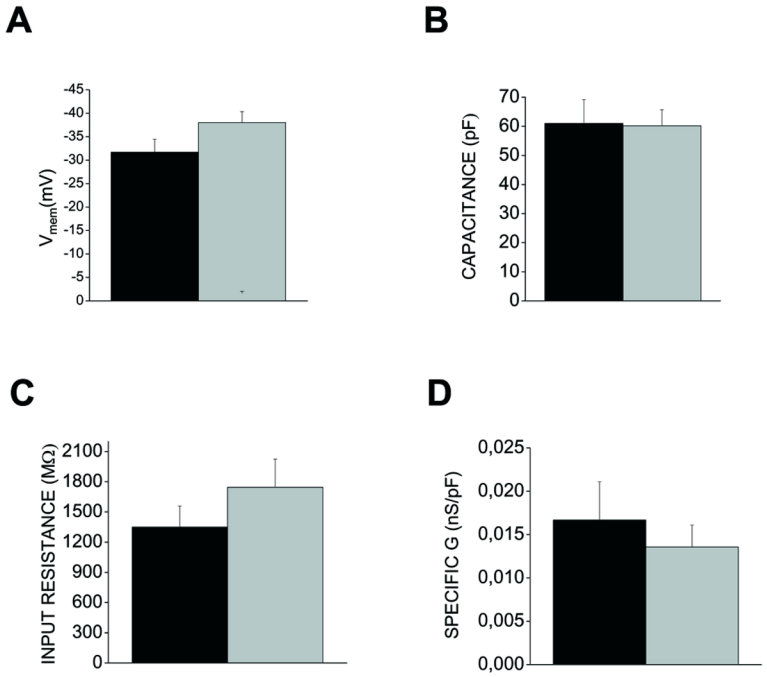

Figure 2.

Summary of electrophysiological properties of astrocytes plated on PDL and silk-coated glass. A) The mean resting membrane potential (Vmem) recorded at a holding potential of -60 mV indicates that astroglial membrane voltage was not significantly different in the two experimental conditions. B) Histogram plot of cell capacitance suggests that cell surface areas were not different in the silk and PDL cells. C) Plot of the mean input resistance (Mohm) of cell types of the two conditions. D) Mean specific conductance in each cell type. No significant difference was observed between properties recorded in astrocytes grown on poly-D-lysine (black bar), and silk (gray bar) (n=10 for poly-D-Lysine seeded and n=19 for silk-seeded astrocytes, $p>0.05$, Independent t-test)

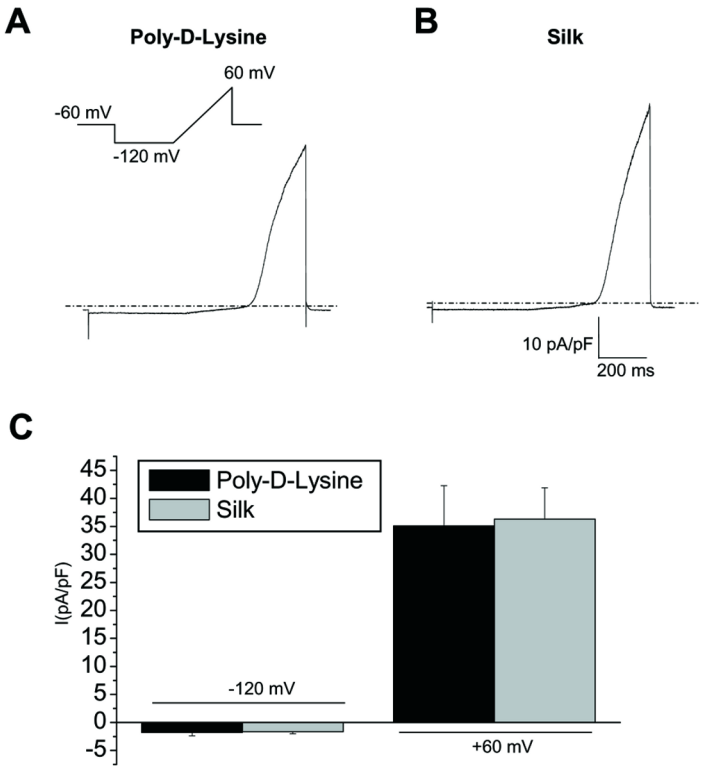

Figure 3.

A-B) Current traces recorded stimulating astrocytes with a voltage ramp protocol from Vh of -60 mV, from -120 to +60 mV (600 ms), after a 500-ms-long step potential to -120 mV (inset), indicate that in astrocytes (left) plated on poly-D-lysine coated glass only voltage-dependent outward rectifying K^+ currents are elicited at potentials more positive than -40 mV. (B) The current profile of astrocytes plated on silk coated coverslips were comparable. C) Histogram plot of current density recorded at -120 mV and +60 mV in two experimental conditions revealed that no significant difference was detected on poly-D-lysine (black bars) and silk-plated cells (gray bars) for inward and outward currents. (n=10 for poly-D-Lysine coated and n=26 for silk-plated cells, $p>0.05$, Independent t-test).

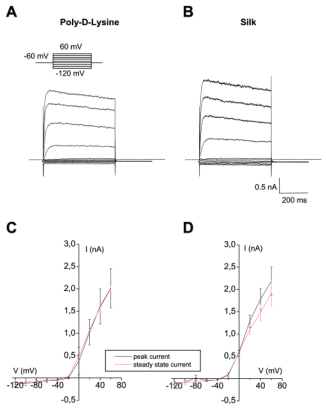

Figure 4.

Representative current traces evoked in astrocytes with a family of voltage steps from Vh of -60 mV, from -120 to 60 mV in 20 mV increments (inset). Typical currents depicting K^+ current are evoked in poly-D-lysine astrocytes (A) and silk-treated astrocytes (B) at potential more positive than -40 mV. The currents had an instantaneous activation and did not display time-dependent inactivation in either experimental condition. C-D) I-V plot: Mean of current intensity recorded at peak (black lines) and steady state (red lines) in poly-D-lysine astrocytes (C) and silk-plated astrocytes (D). The outward potassium current has voltage- and time-dependence comparable in both experimental conditions and resembles those of delayed rectifier potassium channels. (n=4 for poly-D-Lysine coated and n=4 for silk).

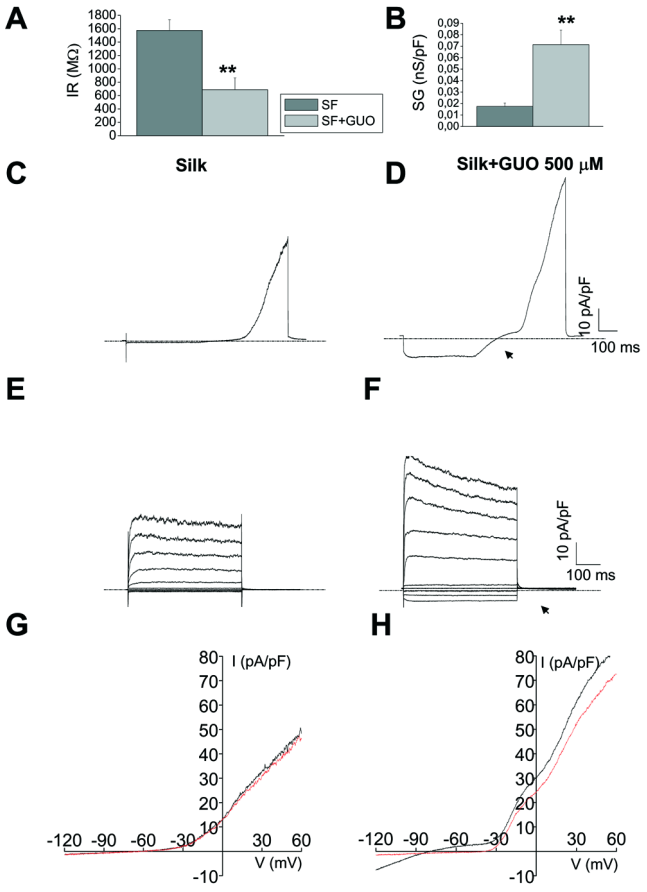

Figure 5.

A-B) Passive properties of cells plated on silk and silk+GUO. A:Histogram of the mean values of input resistance (IR) in untreated (n =26, gray bar) and Guo-treated astrocytes (n = 20, light gray bar). B:histogram plot of the mean normalized conductance (specific G, SG) showing a five-fold increase in Guo-treated cells compared to untreated silk-cells (n =20) **$p < 0.01$ (Student's t-test). C-D). Typical current traces evoked from a holding potential (Vh) of -60 mV stimulating astrocytes with a voltage ramp from -120 to +60 mV (1000 ms), after a 500-ms-long step potential to -120 mV (inset to Fig 3A), indicate that in astrocytes (left) plated on silk displayed only voltage-dependent outward rectifying K^+ conductance (Figure 3). (E-F) Current profile of astrocytes plated on silk+GUO coated coverslips. Note that in response to hyperpolarizing stimulus and inward conductance (arrowhead) is displayed only by silk+GUO treated cells in D and F.

G-H) Typical IV current plot of ramp current traces elicited in silk cells (G) and silk+GUO cells (H) before (black trace) and after (red trace) extracellular superfusion of submillimolar concentrations of barium (Ba^{2+}, 200 μM). Note inhibition by Ba^{2+} of currents elicited at potentials between -80 and -40 mV when the delayed rectifier K^+ current was not activated. Also outward currents in Guo-treated astrocyte were also partially inhibited, suggesting weak rectification profile of K_{ir} conductance.

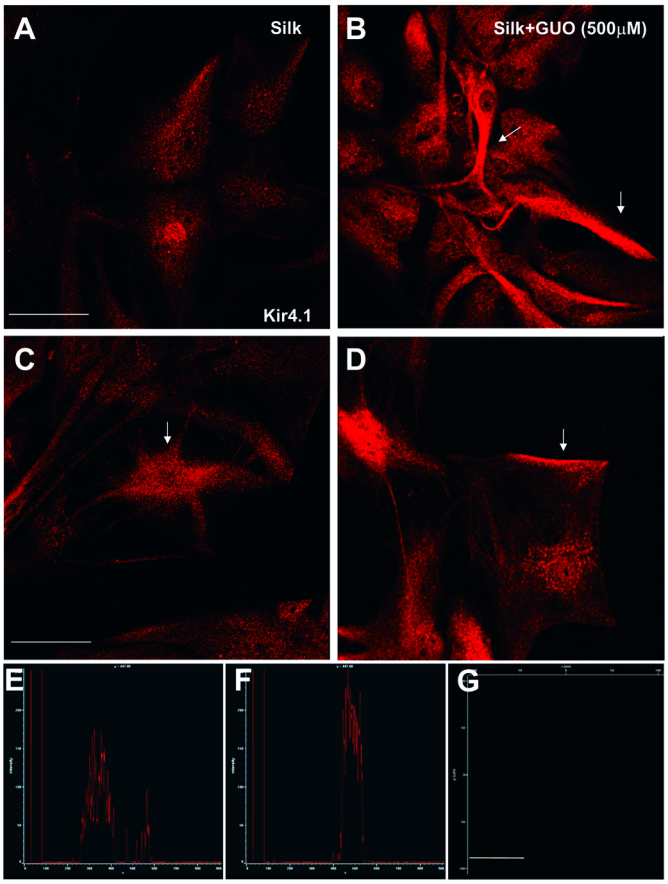

Figure 6.

Single plane confocal image of astroglial cells stained for anti-$K_{ir}4$. Note lower immunosignal intensity indicating low expression level of $K_{ir}4.1$ in plane silk coated cells (A) compared to silk+GUO plated cells (B). C-D) High magnification single plane confocal images of cells revealed that in silk plated cells K_{ir} expression pattern was more mislocalized explaining absence of current upon this experimental condition. On the contrary higher and membrane polarized expression pattern of $K_{ir}4.1$(arrows) can be observed in cells plated on silk film embedded with guanosine (D). E-F Graph plot of fluorescence intenstity (pixel) in μm spatial range analyzed from silk astrocyted (E) and silk+GUO cells (F). Note higher immunofluorescence specificity of K_{ir} 4.1 immunosignal for silk+GUO cells (F). Scale bar is 50 μm. G) Secondary antibody specificity control. Single plane confocal image of immunofluorescent experiment performed without addition of primary-antibody of immunofluorescence. Note that no immunofluorescent signal was observed, supporting the specificity of the assay.